Available online at www.sciencedirect.com

ScienceDirect

Proceedings of the Combustion Institute 39 (2023) 3467–3477

Proceedings of the Combustion Institute

www.elsevier.com/locate/proci

Experimental investigation of NOx emission and ash-related issues in ammonia/coal/biomass co-combustion in a 25-kW down-fired furnace

Peng Ma, Qian Huang*, Tong Si, Yuanping Yang, Shuiqing Li

Key Laboratory for Thermal Science and Power Engineering of Ministry of Education, Department of Energy and Power Engineering, Tsinghua University, Beijing, 100084, China

Received 6 January 2022; accepted 22 July 2022
Available online 24 September 2022

Abstract

Co-firing ammonia in coal units is a promising approach for the phasedown of coal power. In this paper, we demonstrate the feasibility of burning ammonia with coal and biomass in a 25- kW down-fired furnace with a swirl-stabilized burner. Ammonia is injected from the central tube at thermal ratios ranging from 0 to30% and can be completely burnt out in most co-firing cases. We investigate the NO_x emission, unburnt carbon in fly ash, particulate matter formation and ash deposition behaviors when co-firing NH_3 with either SH lignite coal or the coal/biomass blend. With a fixed air staging ratio, the NO_x emission increases linearly with the NH_3 fuel ratio. By increasing the percentage of secondary air, the emitted NO_x can be reduced to 300 ppm with an NH_3 thermal ratio of 30%. The unburnt carbon is affected by NH_3 addition in a complex manner. With a 30% (thermal) NH_3 addition, the unburnt carbon increases from 0.4% to 5.6% for the SH coal mainly due to a temperature drop, but decreases from 2.2% to 0.7% for the SH coal/biomass blend. As for the ash-related issues, the addition of NH_3 to either coal or coal/biomass blend is found to alleviate both the fouling intensity and the ultrafine particulate matter formation ability. This is a major advantage over biomass combustion.

Keywords: Ammonia/coal/biomass; Co-combustion; NOx emission; Air staging ratio; Ash formation and deposition

1. Introduction

There is a worldwide consensus on the phase-down of unabated coal power to reduce carbon emission [1]. The year 2020 sees a plummet by 5% from 2019 levels in the global coal demand [2], but coal still provides 27.2%, the second-largest ratio, of the world's primary energy consumption [3]. In many developing countries the ratio is even higher (e.g., China 56.6%, India 54.8%, Vietnam 51.4%, Indonesia 40.2%, 2020) [3]. Besides, the output of thermal power can be controlled actively and flexibly to stabilize the grid with a rapidly growing penetration of intermittent renewables [4]. Indeed, coal power in developing countries like China has been playing the role of peak shaving for years [4]. Therefore, instead of shutting down the existing units,

* Corresponding author.
E-mail address: huangqian@tsinghua.edu.cn (Q. Huang).

https://doi.org/10.1016/j.proci.2022.07.223
1540-7489

switching to carbon-neutral fuels is believed as a more economical and environmentally-benign approach.

Ammonia (NH_3) and biomass are among the most promising candidates for this purpose. Co-firing biomass with coal has been widely studied and used especially in Europe [5]. In China, some coal plants are retrofitted for co-firing biomass ($\leq$10% of the full power) but frequently run with greater fuel ratios of biomass at reduced outputs. However, the availability issue limits the biomass usage scale, and the severe fouling propensity in biomass combustion remains challenging [6,7].

NH_3, by contrast, obtains more and more attention recently for its great potential as a large-scale and long-duration energy carrier. Now, NH_3 is gradually becoming an indispensable portion of the hydrogen industry with mature technology of global transport and storage at scale [8,9]. Burning NH_3 in coal plants relies on NH_3 costs and combustion technology. The electricity cost of co-firing coal with 20% NH_3 (thermal input) is projected as 150 USD/MWh (China, without CCS, our own estimation) and 180 USD/MWh (Japan, with CCUS), which is compared with 167 USD/MWh (Japan) and 228 USD/MWh (Europe) for coal power equipped with CCUS [10,11].

With a cost-competitive prospect, co-firing NH_3-coal has been tested on a 1.2 MW furnace (NH_3 fuel ratio from 0 to 100% with various feeding modes) [12] and a 155 MW boiler (NH_3 fuel ratio 0.6%) [13]. Generally, little NH_3 slip is detected, and the NO_x emission is increased to a mild extent with the NH_3 fuel ratio no greater than 20%. The same trend is observed in a numerical study on the full-scale furnace [14]. These efforts alleviate the NO_x concerns at least for co-firing NH_3 with a small fuel ratio. As a common species for fuel-N transformation in pulverized coal combustion, NH_3 itself is an effective NO reduction agent [15]. It is recently found that the NH_3 co-firing synergistically promotes NO heterogeneous reduction with char [16]. Therefore, the key to control NO_x in an industrial NH_3-coal swirl flame seems to effectively 'trap' NH_3 long enough in the volatile-rich region [8,9,12,17]. It must be achieved through elaborate manipulation of the fuel-air mixing strategy.

However, many issues on practical NH_3-solid fuel co-combustion remain controversial or unclear: First, little is known about the NH_3 influence on mineral ash formation and deposition, the key factor affecting the safety of heating surfaces in the boiler. Secondly, as pointed out in Ref. [9], the reported unburned carbon fractions in fly ashes after NH_3 addition seem to be inconsistent in the literature. Then, co-firing NH_3 with biomass (or coal-biomass blends) has been rarely studied, even though it may as well become practical. Last, decision-makers of the coal plant may want to know about the limit of the unit to burn NH_3 without any system retrofit.

We note that the 20$\sim$100-kW furnaces are well suited to fill the research gap because coal burns out with time-temperature histories and particle concentrations similar to those in practical boilers and the scale of these furnaces still allows precise and reproducible operating conditions for mechanistic studies [18–20]. Recent progress in simultaneous characterization of the fly ash and deposits [21–23], as well as the flexibility of the furnace to fuel types, makes it possible to delve into NH_3-coal/biomass co-combustion performance, but it has not been reported yet.

The objective of this work is to elucidate the combustion performance in co-firing NH_3 with coal/biomass in a 25-kW quasi-one-dimensional self-sustained down-fired furnace. Ammonia is centrally fed into a swirl coal burner. A set of well-designed conditions are achieved to study: (i) ash-related issues; (ii) NH_3-coal-biomass co-combustion and the effects to, among others, the unburnt carbon; (iii) the limit of burning NH_3 on conventional swirl burners with little structural retrofit. We reveal the NO_x emissions and unburned carbon in fly ashes under various NH_3 fuel ratios (up to 30% thermal) and secondary air ratios. Ammonia slip is generally negligible. The fouling propensity and fine particle size distributions are reported for the first time in the NH_3-coal-biomass system.

2. Experimental apparatus and methods

2.1. Fuel property

In this work, we use SH lignite coal, the design coal of a 2000-MW unit located in the northwest of China. A corn straw (denoted CS) is chosen as the biomass to be mixed uniformly with coal. The thermal ratio of CS is set as 20% (higher than 10% to better mimic the real situation and further manifest the biomass effect), with the blend denoted SH:CS=4:1. Table 1 lists the fuel properties. Note that the blend has higher volatile and fewer ash contents than SH coal. Greater Na and K fractions are present in the blend, which may affect the ash behaviors [22,24–26]. Fig. 1 shows the volumetric particle size distributions of the raw fuel samples measured by a Malvern (Master sizer 2000). It is found that the mean size of CS is about 3 times of SH coal due to the weaker grindability of biomass. Table 2 lists the feed rates of SH and the blend in the experiments with the NH_3 fuel ratios set as 0, 0.1, 0.2, and 0.3.

2.2. 25-kW down-fired furnace and sampling methods

The combustion experiments are performed in a 25-kW self-sustained, quasi-one-dimensional

Table 1
Properties of SH lignite and the blend (SH: CS=4:1).

	SH	SH: CS=4:1
Proximate analysis (wt.%, dry basis)		
Fixed carbon	45.10	39.51
Volatile matter	32.96	42.99
Ash	21.94	17.50
HHV (MJ/kg)	19.30	18.66
Ultimate analysis (wt.%, dry, ash-free basis)		
C	50.49	48.42
H	4.12	4.34
N	0.88	0.82
S_{total}	0.72	0.56
O (by difference)	43.85	45.86
ash composition (wt%)		
SiO_2	39.62	38.41
Al_2O_3	16.29	14.70
Fe_2O_3	9.21	8.98
CaO	15.25	15.78
MgO	4.21	4.23
TiO_2	0.95	0.98
SO_3	9.35	9.32
P_2O_5	0.10	0.24
K_2O	2.06	3.67
Na_2O	1.73	1.87
$d_{0.5}$ (μm)	33.09	106.73

Table 2
Feed rates of SH coal and the blend in the experiments.

NH_3 fuel ratio (thermal)	SH (kg/h)	SH: CS=4:1 (kg/h)	Overall air ratio
0.0	4.07	4.18	1.3
0.1	3.66	3.76	1.3
0.2	3.26	3.34	1.3
0.3	2.85	2.93	1.3

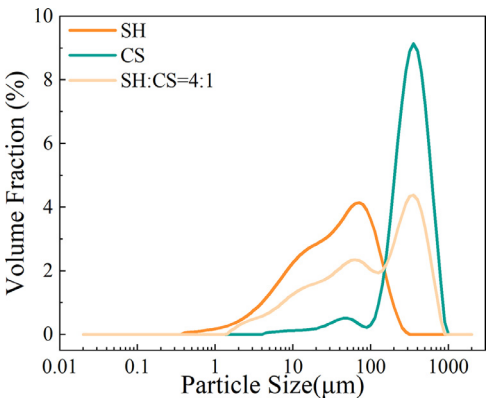

Fig. 1. Volumetric particle size distribution of SH lignite, CS biomass, and the blend (SH: CS=4:1).

down-fired furnace as exhibited in Fig. 2. The structure and operation procedures of the furnace are detailed in our previous work [20,22]. The refractory lining of the furnace is made of silicon carbide high-temperature ceramic, calcium silicate board and aluminum silicate fiber felt. The inner diameter of the furnace is 150 mm. The total height is 3800 mm. The flue gas flows pass a treatment system before entering the stack. Four sampling ports denoted P1-P4 are designed for fly ash and deposit sampling, with the temperatures monitored by S-type thermocouples. In particular, the residence time in P4 (2660 mm away from the burner) is ~1.5 s to ensure the fuel burnout. Before the experiments, the sealing of the furnace was carefully examined to prevent NH_3 leak.

A multi-fuel burner equipped on the furnace top is shown in Fig. 2a. The burner consists of four outside- in coaxial tubes, including the swirled secondary air preheated to 380 °C, the primary air carrying pulverized solid fuels (coal or biomass) to be fed into the furnace through the annular port, the liquefied petroleum gas (LPG) for warming up the furnace to be injected from annular-placed small holes, and the central tube for gaseous NH_3 injection. The NH_3 nozzle is fixed at 16 mm.

The flue gas compositions including NO_x (NO, NO_2 and N_2O), CO, CO_2, O_2 and SO_2 are measured by two gas analyzers (MRU-VARIO PLUS)

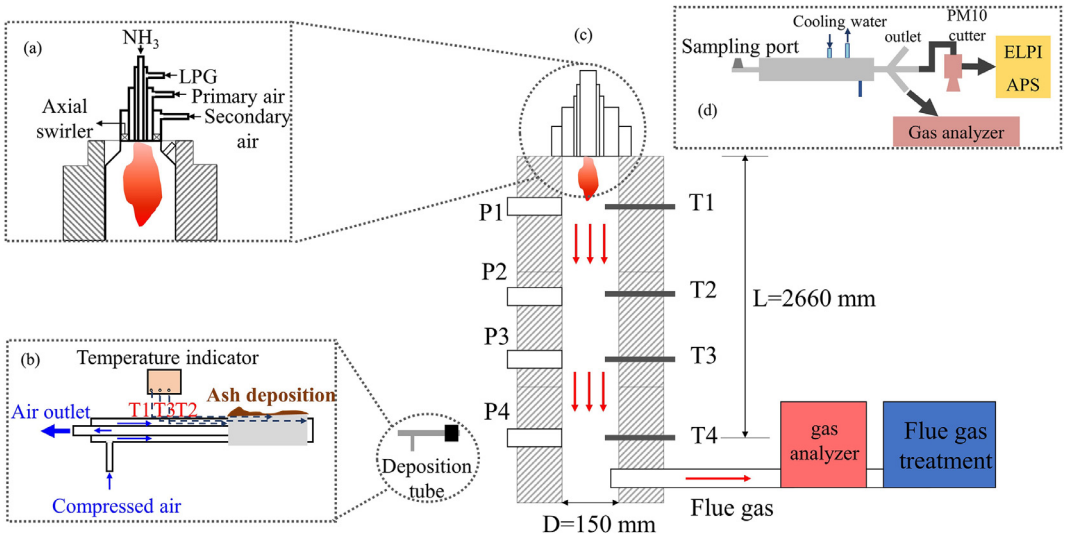

Fig. 2. Schematic of the 25-kW down-fired furnace: (a) The swirl burner adapted to central NH_3 injection; (b) Deposition probe; (c) The furnace with sampling ports P1-P4 and temperature monitors T1-T4; (d) Fly ash sampling probe.

upstream of the gas treatment system (see Fig. 2c). The sampling lines are heated above 120°C to prevent water condensation and NO_2 dissolution. Another analyzer (Gasmet DX4000) is used to measure ammonia slip at the outlet of the furnace.

The ash deposits and fly ash samples are collected at P4 of the furnace. The deposition probe (see Fig. 2b) has a removable sleeve of Φ20 mm × L 50 mm with the surface temperature controlled at 600°C by compressed air. The sleeves are heated to 900°C before experiments to eliminate the oxidation-induced mass changes [20]. The sleeves are measured before and after deposition experiments for a certain elapsed time to record the deposited mass.

The fine particle sampling probe (see Fig. 2d) uses two stages of dilution to minimize the errors induced by the aspiration sampling [20]. The overall dilution ratio is ~ 150 (using CO_2 as the indicator). The particle size distributions are measured, respectively, by the APS (TSI Inc., aerodynamic diameter 0.5–20 μm) and ELPI+ (Dekati, aerodynamic diameter 0.017–10 μm, under DLPI mode). The flue gas flows through a PM_{10+} cutter before entering ELPI+. The bulk ash trapped in the cutter is collected for TGA (TGA Q500) analysis to 1000 °C to determine the unburned carbon.

In the experiments, a high-temperature-resistant camera is inserted into P2 to record the top flames, as shown in Fig. 3a for various fuels. The type I jet-like swirl flame [27] is formed in experiments (as shown in Fig. 3a, the flame is mainly located in the center of the furnace). The temperature profiles along the furnace are presented in Fig. 3b and are quite close among various fuels. The temperature at P4 is ~750°C.

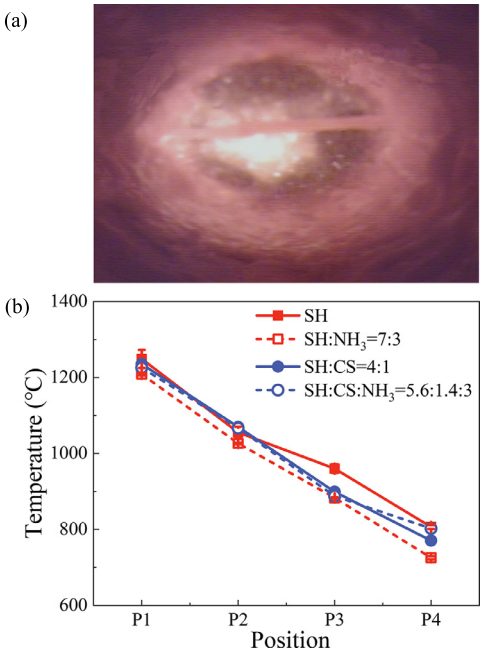

Fig. 3. (a) Typical top-view flame image (exposure time: 1/2000s); (b) Temperature profiles along the furnace for burning different fuels.

3. Results and discussion

3.1. Ammonia slip and flue gas compositions from a continuous test

Fig. 4 presents the flue gas compositions during a series of fuel-switching operations in the furnace. LPG is first used to warm up the furnace to

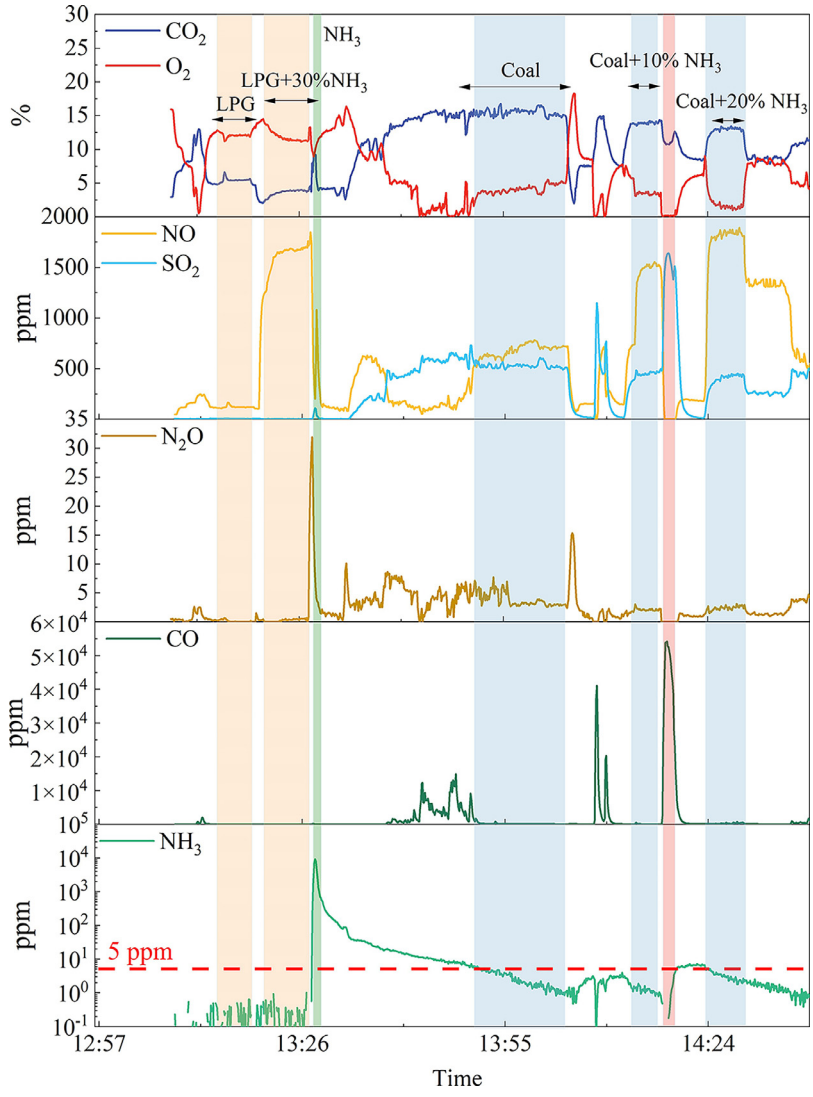

Fig. 4. Flue gas compositions during a series of continuous fuel switching operations.

reach stable conditions (~1250°C at P1), producing the flue gas NO about 100 ppm and almost no SO_2. Then we switch to co-firing LPG with 30%-thermal NH_3. Once ammonia is added, the NO_x emission largely increases to ~1700 ppm. No ammonia slip is detected. We further test pure NH_3 combustion by cutting down the LPG supply and increasing the NH_3 flow rate to ~12 kW. Unfortunately, this leads to a serious NH_3 slip over 10^4 ppm and a NO emission ~1000 ppm, which is lower than LPG+30% ammonia and results from the NO reduction by SNCR reactions with sufficient NH_3 supply [8,28]. We have to cut off NH_3 immediately and re-supply LPG until the monitored NH_3 slip drops below 5 ppm. Then LPG is switched to pure SH coal, yielding flue gas CO_2, O_2, NO, SO_2 and CO as ~16%, ~5%, ~700 ppm, ~500 ppm and ~100 ppm, respectively. Further increasing NH_3 fuel ratio to 20% results in even lower CO_2 and SO_2, and NO increases to ~1800 ppm. The ammonia slip is always less than 5 ppm in co-firing NH_3-coal, verifying that NH_3 slip may not be a serious concern [14,29]. But the NO issue is vital.

Besides, the potent greenhouse gas nitrous oxide (N_2O) can be formed from ammonia combustion [8,9]. As shown in Fig. 4, when cofiring NH_3 with LPG or coal, flue gas N_2O is no higher than 2.5 ppm, far lower than NO (~1500 ppm). During pure NH_3 combustion test, though, a notable N_2O emission (~30 ppm) is recorded along with the serious ammonia slip, which indicates that N_2O can be an issue of concern. No direct correlations can be

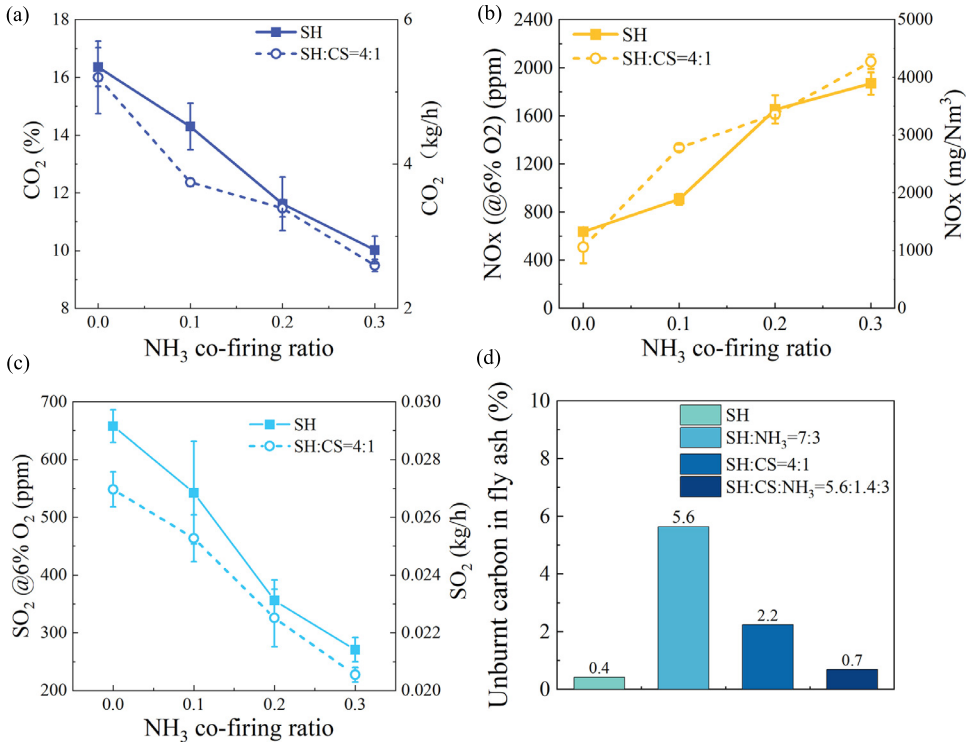

Fig. 5. CO_2, SO_2, NO_x emission and unburnt carbon in the fly ash at different ammonia co-firing ratios.

inferred between N_2O and NO (or O_2, NH_3, etc.) concentrations from the data. The N_2O formation mechanism and its greenhouse effect in NH_3 combustion thus demand further research efforts.

3.2. CO_2, SO_2, NO_x emission, and unburnt carbon in fly ash

Fig. 5 illustrates the measured CO_2, SO_2, NO_x emission and unburnt carbon in the fly ash. To exclude the dilution effect, we calculate the mass emission rates (kg/h) of CO_2 and SO_2 based on the flue gas flow rates and the gas compositions. Because NH_3 is free of carbon and sulfur, the measured CO_2 (Fig. 5a) and SO_2 (Fig. 5c) emissions decline linearly with the NH_3 co-firing ratio for both SH coal and the blend (SH: CS=4:1). It highlights the positive effects of co-firing ammonia on carbon reduction. In addition, the blend (SH: CS=4:1) produces less SO_2 emission than pure SH coal combustion because the biomass CS has a lower sulfur content (see Table 1).

In contrast, the NO_x emission in Fig. 5b increases almost linearly with the NH_3 co-firing ratio for both SH coal and the blend (SH: CS=4:1), provided that the air staging strategy and the excess O_2 concentration are kept the same. Recall that we have jet-like swirl flames in the experiments (Fig. 3a) and NH_3 was fed in as a central jet. Therefore, the higher blending ratio of NH_3 leads to larger central fuel jet intensities and reduces the residence time of NH_3 in the fuel rich zone. With less extents of decomposition, NH_3 experiences a quicker entry into the oxidation zone where the fuel-N conversion into NO becomes active. It suggests the challenge the fuel-N in NH_3 poses to existing combustion facilities. For instance, our 25-kW furnace, without considerable modification of the burner, can only adopt an NH_3 co-firing ratio no greater than 10% with SH coal to ensure a flue gas $NO_x \leq 1000$ ppm, a concentration that can be effectively handled by current SCR systems.

We further characterize the unburnt carbon in the fly ash at sampling P4 in cases of 30%-thermal NH_3, with results shown in Fig. 5d. For SH coal, a 30%-thermal NH_3 addition increases the fraction of unburnt carbon in the fly ash from 0.4% to 5.6%. The blend (SH: CS=4:1) features a larger value (2.2%) of unburnt carbon than pure SH coal, which can be interpreted by the much coarser particles of biomass CS (see Fig. 1). However, a 30%-thermal NH_3 addition to the blend reduces the unburnt carbon to 0.7%, though still larger than that of SH coal. While several previous studies report inconsistent results of NH_3 effect on coal burnout [12,14,17,29], our work reveals opposite trends from a single set of experiments burning different fuels, demonstrating that several factors with

distinct consequences should be taken into consideration.

As compared with pure SH coal, adding 30%-thermal NH_3 may substantially reduce the temperature. The adiabatic flame temperature of NH_3 (~1800°C [8]) is far lower than the burning temperature of coal/char (~2000–2400°C [30]). Moreover, the previous study shows that when NH_3 co-firing ratio reaches 20% (thermal), the flame zone (FZ) temperature drops about 200°C, whereas the post flame temperatures drop about 50°C [14]. Hence, it is believed that with NH_3 addition, the temperature difference in the flame zone (even upstream of P1) is remarkably greater than the 40–100°C shown in Fig. 3b. Besides, NH_3 combustion could be more efficient in consuming oxygen and slows down the coal/char oxidation in flame zone. Both factors contribute to the increased unburnt carbon fraction for NH_3-SH coal co-combustion.

For the blend (SH: CS=4:1), NH_3 co-firing from the central jet is likely to reduce the concentration of larger fuel particles and promote the mixing of solid fuel particles with combustion air, resulting in the improved burnout under the fixed air staging ratio [12]. Nevertheless, we remark that future in-depth investigations are needed to clarify this issue.

3.3. Manipulating air staging ratio to minimize NO_x emission

Whether NH_3 acts as the NO_x contributor or NO reductant heavily relies on the local atmosphere and the NH_3 injection approach [8,9,12,14,29]. Thus, adjusting the air staging ratio can be a convenient way to change the local condition without physical modifications of the system. In this work, we adjust the solenoid valve controlling the secondary air flow rate and percentage during co-firing 30%-thermal NH_3 with SH coal. Notice that the primary air valve is left unchanged. It leads to changes in the total flow rate and major gaseous emissions, as shown in Fig. 6. We see that by reducing the secondary air percentage from 64% to 16%, NO_x emission is remarkably mitigated from 2000 ppm to 300 ppm, while the excess O_2 changes mildly (reduced from 8% to 4%). SO_2 and CO increase from 300 to 500 ppm, and from 40 to 200 ppm, respectively. The reduction of NO_x emission may be primarily attributed to the lowered overall air ratios caused by the decreased secondary air ratio and a constant fuel supply. The less oxidizing environment, as indicated by elevated CO concentrations (see Fig. 6), suppresses the radical pool of OH, O, etc., and weakens the intensity of NO_x formation through the fuel-N pathway [8,31]. Note that the NO_x emission of 300 ppm is even lower than pure SH coal combustion (without adjusting the air staging ratio). We need to mention that air staging manipulation has been proved effective for NO_x reduction in both pure ammonia combustion [12] and ammonia/nature gas co-combustion [32].

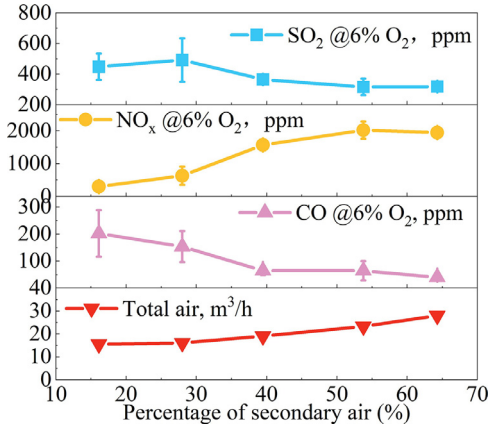

Fig. 6. SO_2, NO, CO emission and total air flow rate v.s. secondary air percentage in co-firing 30%-thermal NH_3 with SH coal.

It implies a powerful way for existing coal units to partially burn NH_3 even with non-optimized physical/structural retrofit.

3.4. Ash deposition

As for the ash-related issue, Fig. 7a illustrates the time evolution (within 1 h) of deposited mass onto the probe. Fig. 7b presents the visual morphologies of the ash deposits. Pure SH coal combustion generates deposits linearly growing with time from 0.22 g at 15 min to 0.77 g at 1 h. By contrast, adding 30%-thermal NH_3 dramatically reduces the deposited mass to 0.45 g at 1 h. When the biomass CS is involved, remarkably more deposits have been collected on the probe than in the SH and SH–NH_3 combustion cases, indicating the enhancing effect of biomass on ash deposition. Meanwhile, except for pure SH, the deposits are collected more slowly at the time interval of 30–60 min than at the 0–30 min period. It could be attributed to the deposit shedding [22]. Stratified deposited layers are observed in Fig. 7b, with a light-colored fine inner layer covering the entire probe and the gray bulk deposits located on the windward side. At larger elapsed times, the ash deposits gain 'rougher' surfaces, implying more frequent 'local shedding' especially for the blend (SH: CS=4:1 without NH_3). When mixing CS with SH, the contents of K and Na in the ash increase, including K from 2.06% to 3.67% and Na from 1.73% to 1.87% (see Table 1). As a result, bulk ash particles become stickier with the formation of AAEM-rich "coating layers" so that they are more prone to stay after impacting the probe [22,33]. The difference in the one-hour deposited masses between NH_3-addition and no-NH_3 cases is caused by the varying extents of shedding [34].

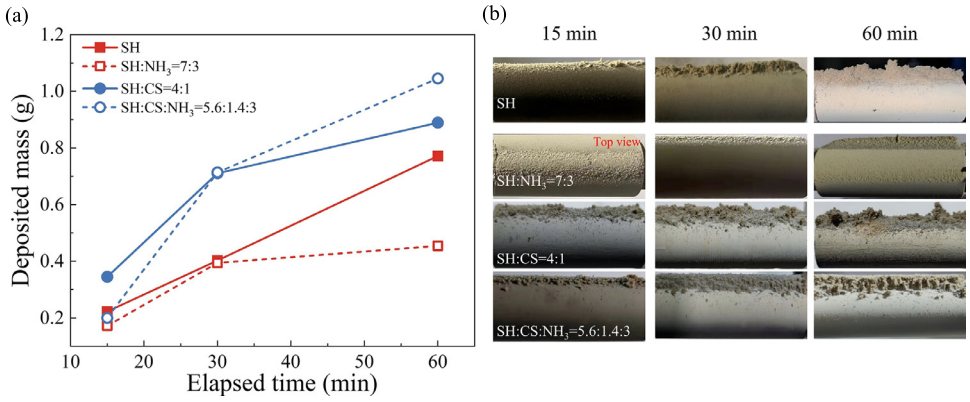

Fig. 7. (a) Time evolution of the deposited mass with elapsed time; (b) Visual morphologies of the deposits.

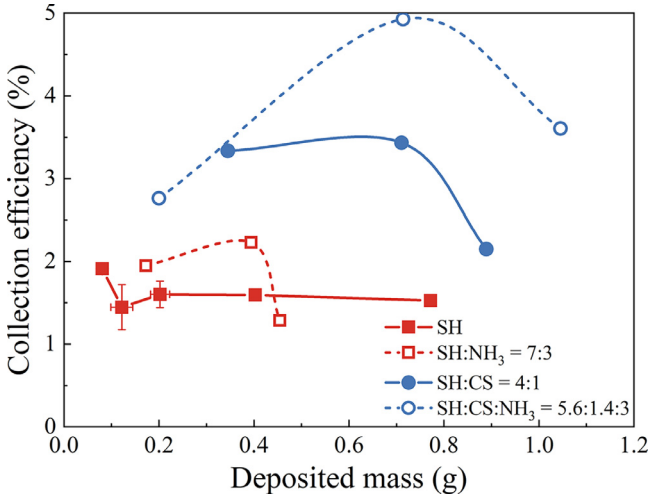

Fig. 8. Collection efficiency as a function deposited mass.

Fig. 8 further shows the normalized ash collection efficiency as a function of the deposited mass. The collection efficiency is defined as the fraction of deposited particles over the total incoming ash onto the projected area of the probe, formulated as $CE(\%) = \dot{m}_d A_c/(\dot{m}_F Y_{ash} A_p)$. Here $\dot{m}_d$ is the ash deposition rate (kg/s) calculated by the ash deposited mass in a certain elapsed time, A_c is the cross-section area of the furnace (m^2), $\dot{m}_F$ is the fuel feed rate (kg/s), Y_{ash} is the ash content in fuels, and A_p is the projected surface area of the sampling probe (m^2) [22,33]. It is a good indicator of the ash deposition propensity. For pure SH coal, the collection efficiency is ~1.5%, a rather small value. Adding 30%-thermal NH_3 leads to small changes that could be explained by the shedding effect (the less coal/ash loading, the less propensity to shed). By contrast, the collection efficiency of co-firing with biomass CS tops 5%, a large value for coals with strong fouling propensities [22]. The contributions of Na and K (with higher contents in the blended fuel, see Table 1) can be reasonably inferred [22,33].

3.5. Particle size distribution of fly ash in the coal burnout regime

Fig. 9a shows the particle size distributions (PSD) of particulate matter (PM) at P4 (the burnout regime) on the basis of unit input ash (mg/g_ash), and Fig. 9b reports the yields of $PM_{0.26}$, PM_1, $PM_{2.5}$ and $PM_{2.5-10}$. We merge the ELPI and APS data in Fig. 9a by converting the number PSDs from APS to the mass PSDs after simply assuming a uniform particle density of 2000 kg/m^3 [35]. We find that a reasonable agreement can be achieved between APS and ELPI+ (or DLPI+) measurements in the overlapping size range (0.5–10 μm) for burning pure SH coal and the SH–NH_3 (30%-thermal) blend. The overall

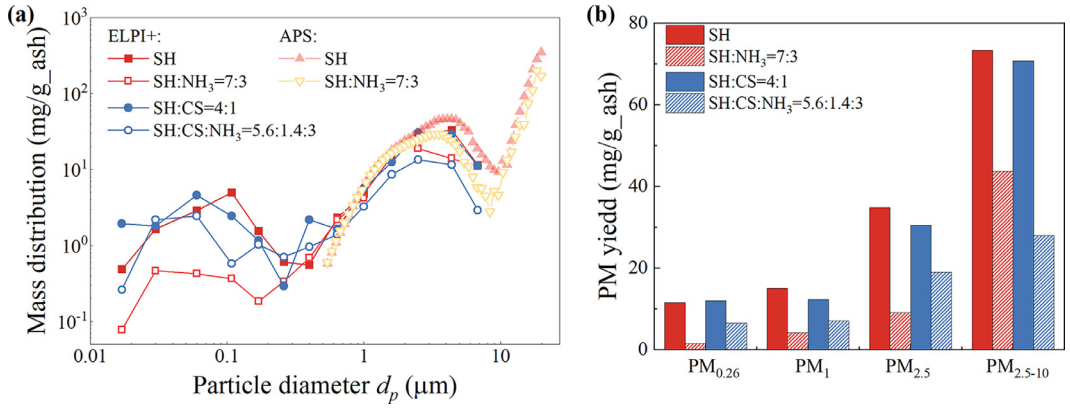

Fig. 9. (a) Particle size distribution (mg/g_ash) and (b) PM yield (mg/g_ash) of fly ash sampled at P4 for burning SH coal, SH-30% (thermal) NH_3 blend, SH–CS blend, and SH–CS-NH_3 blend. The number PSDs from 0.5 to 20 μm measured by APS is converted to mass PSDs by assuming a constant density of 2000 kg/m^3.

mass PSD from solid fuel combustion, even with NH_3 addition, is trimodal: (i) an ultrafine mode finer than 0.1 μm, (ii) a micrometer mode peaked between 1 and 10 μm, and (iii) a coarse mode with the peak size greater than 10 μm (even beyond 20 μm, the detection limit of APS) [36]. Generally, the ultrafine mode is formed by the pathway of nucleation-condensation-coagulation of vaporized minerals, the micrometer mode is mainly formed by the discrete included/excluded minerals via coalescence, fragmentation, et al., and the coarse mode is attributed to the unburnt char and bulk excluded ash in coal [26,36]. A comparison among the fuel types in Fig. 9b helps reveal the influences of NH_3 and biomass blending. In the ultrafine size range, co-firing SH coal with 30%-thermal NH_3 generates less PM, especially $PM_{0.26}$, which accounting for only ~10% of that from SH coal combustion. This seems to be a direct consequence of the lowered temperature (see Fig. 3b) and thus a weakened strength of minerals vaporization-nucleation-condensation. On the contrary, the $PM_{0.26}$ formation ability of the blend (SH: CS=4:1) is greater than pure SH coal (for more than 50%). The more abundant ultrafine particles and the exacerbated fouling tendency indicate the adverse effects of biomass co-firing. The ash-related problems seem to be minor for co-firing ammonia; Instead, the combustion intensity (unburned carbon) and NO_x issues are the central concerns.

4. Conclusions

In this paper, we study the NO_x emission, carbon burnout, and ash-related issues in co-firing NH_3 with coal and biomass in a 25-kW down-fired combustor. By using a conventional swirl burner with central injection of NH_3 (up to 30% thermal input), a complete burnout of NH_3 is achieved with only a trace amout of NH_3 slip detected.

While CO_2 and SO_2 concentrations decline linearly with the NH_3 fuel ratio, the NO_x emission increases instead. Manipulating the air staging ratio by reducing the secondary air percentage is shown effective to reduce NO_x down to ~300 ppm.

For carbon burnout, we show a complex effect of NH_3 addition by increasing the unburnt carbon in fly ashes of coal-NH_3 mixtures while reducing it in cases co-firing coal, biomass and NH_3. The possible mechanisms are discussed.

Co-firing NH_3 with either lignite coal or the coal-biomass blend reduces both the fouling intensity and the ultrafine particulate matter yield, as compared with the opposite influences of biomass co-firing. The observed trends seem to be consistent with the reduced coal feed rate and the temperature variations after NH_3 addition to the furnace.

Our work verifies the feasibility of co-firing NH_3 in existing coal units. Future work should be directed towards more detailed investigations of the air staging strategy and carbon burnout issues.

Declaration of Competing Interest

The authors declare that they have no known competing financial interests or personal relationships that could have appeared to influence the work reported in this paper.

Acknowledgments

This work was mainly funded by the National Natural Science Foundation of China (Grants No. 51725601 and 52006121). The authors are grateful to Prof. Qiang Yao at Xinjiang Univ., Dr Fang Niu

at China Coal Research Institute, and Dr. Ye Yuan at Huaneng group, Dr. Jiankun Zhuo at Tsinghua Univ. for helpful discussions. Special thanks to Mr. Yi Di and Mr. Lulu An for kindly help.

References

[1] The 26th United Nations Climate Change Conference of the Parties (COP26), available at https://unfccc.int/sites/default/files/resource/cma3_auv_2_cover%20decision.pdf.
[2] IEA, coal report 2020, available at https://iea.blob.core.windows.net/assets/00abf3d2-4599-4353-977c-8f80e9085420/Coal_2020.pdf.
[3] BP, Statistical review of world energy 2021, available at https://www.bp.com/content/dam/bp/business-sites/en/global/corporate/pdfs/energy-economics/statistical-review/bp-stats-review-2021-full-report.pdf.
[4] Y.J. Gu, J. Xu, D.C. Chen, Z. Wang, Q.Q. Li, Overall review of peak shaving for coal-fired power units in China, Renew. Sust. Energ. Rev. 54 (2016) 723–731.
[5] M.S. Roni, S. Chowdhury, S. Mamun, M. Marufuzzaman, W. Lein, S. Johnson, Biomass co-firing technology with policies, challenges, and opportunities: a global review, Renew. Sust. Energ. Rev. 78 (2017) 1089–1101.
[6] S.G. Sahu, N. Chakraborty, P. Sarkar, Coal-biomass co-combustion: an overview, Renew. Sust. Energ. Rev. 39 (2014) 575–586.
[7] U. Kleinhans, C. Wieland, F.J. Frandsen, H. Spliethoff, Ash formation and deposition in coal and biomass fired combustion systems: progress and challenges in the field of ash particle sticking and rebound behavior, Prog. Energy Combust. Sci. 68 (2018) 65–168.
[8] H. Kobayashi, A. Hayakawa, K.D. Kunkuma, A. Somarathne, C Ekenechukwu, Oka for, Science and technology of ammonia combustion, Proc. Combust. Inst. 37 (2019) 109–133.
[9] A. Valera-Medina, F. Amer-Hatem, A.K. Azad, I.C. Dedoussi, M. de Joannon, R.X. Fernandes, P. Glarborg, H. Hashemi, X. He, S. Mashruk, J. McGowan, C. Mounaim-Rouselle, A. Ortiz-Prado, A. Ortiz-Valera, I. Rossetti, B. Shu, M. Yehia, H. Xiao, M. Costa, Review on ammonia as a potential fuel: from synthesis to economics, Energy Fuels (2021).
[10] K. Hiraoka, Y.W. Fujimura, M. Kai, K. Sakata, Y. Ishimoto, Y. Mizuno, Cost evaluation study on CO2-free ammonia and coal Co-fired power generation integrated with cost of CCS, Report No.434c, 2018 AIChE Annual Meeting, Pittsburgh, US, 2018.
[11] A. Valera-Medina, H. Xiao, M. Owen-Jones, W.I.F. David, P.J. Bowen, Ammonia for power, Prog. Energy Combust. Sci. 69 (2018) 63–102.
[12] M. Tamura, T. Gotou, H. Ishii, D. Riechelmann, Experimental investigation of ammonia combustion in a bench scale 1.2 MW-thermal pulverised coal firing furnace, Appl. Energy 277 (2020).
[13] H. Tanigawa,Test results of the ammonia mixed combustion at mizushima power station unit no.2 and related patent applications, Report No.549a, 2018 AIChE Annual Meeting, Pittsburgh, US, 2018.
[14] S. Ishihara, J. Zhang, T. Ito, Numerical calculation with detailed chemistry on ammonia co-firing in a coal-fired boiler: effect of ammonia co-firing ratio on NO emissions, Fuel 274 (2020) 117742.
[15] A. Shamooni, P. Debiagi, B.S. Wang, T.D. Luu, O.T. Stein, A. Kronenburg, G. Bagheri, A. Stagni, A. Frassoldati, T. Faravelli, A.M. Kempf, X. Wen, C. Hasse, Carrier-phase DNS of detailed NOx formation in early-stage pulverized coal combustion with fuel-bound nitrogen, Fuel 291 (2021).
[16] P. Chen, Y. Fang, P. Wang, M. Gu, K. Luo, J. Fan, The effect of ammonia co-firing on NO heterogeneous reduction in the high-temperature reduction zone of coal air-staging combustion: experimental and quantum chemistry study, Combust. Flame 237 (2022).
[17] Akira Yamamoto, Masayoshi Kimoto, Yasushi Ozawa, S. Hara,Basic co-firing characteristics of ammonia with pulverized coal in a single burner test furnace, Report No.542a, 2018 NH3 Fuel Conference, Pittsburgh, US, 2018.
[18] W.J. Morris, D. Yu, J.O.L. Wendt, Soot, unburned carbon and ultrafine particle emissions from air- and oxy-coal flames, Proc. Combust. Inst. 33 (2011) 3415–3421.
[19] Q. Huang, P. Ma, Q. Gao, S.Q. Li, Ultrafine particle formation in pulverized coal, biomass, and waste combustion: understanding the relationship with flame synthesis process, Energy Fuels 34 (2020) 1386–1395.
[20] J.K. Zhuo, S.Q. Li, Q. Yao, Q. Song, The progressive formation of submicron particulate matter in a quasi one-dimensional pulverized coal combustor, Proc. Combust. Inst. 32 (2009) 2059–2066.
[21] Z.H. Zhan, A.R. Fry, J.O.L. Wendt, Deposition of coal ash on a vertical surface in a 100kW downflow laboratory combustor: a comparison of theory and experiment, Proc. Combust. Inst. 36 (2017) 2091–2101.
[22] G. Li, S. Li, Q. Huang, Q. Yao, Fine particulate formation and ash deposition during pulverized coal combustion of high-sodium lignite in a down-fired furnace, Fuel 143 (2015) 430–437.
[23] Z. Liu, J.B. Li, Q.H. Wang, X.F. Lu, Y.Y. Zhang, M.M. Zhu, Z.Z. Zhang, D.K. Zhang, An experimental investigation into mineral transformation, particle agglomeration and ash deposition during combustion of Zhundong lignite in a laboratory-scale circulating fluidized bed, Fuel 243 (2019) 458–468.
[24] J.C. Van Dyk, S.A. Benson, M.L. Laumb, B. Waanders, Coal and coal ash characteristics to understand mineral transformations and slag formation, Fuel 88 (2009) 1057–1063.
[25] X. Wu, X. Zhang, K. Yan, N. Chen, J. Zhang, X. Xu, B. Dai, J. Zhang, L. Zhang, Ash deposition and slagging behavior of Chinese Xinjiang high-alkali coal in 3 MWth pilot-scale combustion test, Fuel 181 (2016) 1191–1202.
[26] Q. Gao, S. Li, Y. Xu, J. Liu, A general mechanistic model of fly ash formation during pulverized coal combustion, Combust. Flame 200 (2019) 374–386.
[27] R.-H. Chen, J.F. Driscoll, J. Kelly, M. Namazian, R.W. Schefer, A comparison of bluff-body and swirl-stabilized flames, Combust. Sci. Technol. 71 (1990) 197–217.

[28] J.-H. Park, J.-W. Ahn, K.-H. Kim, Y.-S. Son, Historic and futuristic review of electron beam technology for the treatment of SO2 and NOx in flue gas, Chem. Eng. J. 355 (2019) 351–366.
[29] J. Zhang, T. Ito, H. Ishii, S. Ishihara, T. Fujimori, Numerical investigation on ammonia co-firing in a pulverized coal combustion facility: effect of ammonia co-firing ratio, Fuel 267 (2020) 117166.
[30] R. Khatami, Y.A. Levendis, An overview of coal rank influence on ignition and combustion phenomena at the particle level, Combust. Flame 164 (2016) 22–34.
[31] H. Lee, M.-J. Lee, Recent advances in ammonia combustion technology in thermal power generation system for carbon emission reduction, Energies 14 (2021).
[32] Japan Science and Technology Agency, available at https://www.jst.go.jp/pr/announce/20161031-2/, (in Japanese).
[33] X.G. Xu, S.Q. Li, G.D. Li, Q. Yao, Effect of Co-firing straw with two coals on the ash deposition behavior in a down-fired pulverized coal combustor†, Energy Fuels 24 (2010) 241–249.
[34] Q. Huang, Y. Zhang, Q. Yao, S. Li, Mineral manipulation of Zhundong lignite towards fouling mitigation in a down-fired combustor, Fuel 232 (2018) 519–529.
[35] S. Andini, R. Cioffi, F. Colangelo, T. Grieco, F. Montagnaro, L. Santoro, Coal fly ash as raw material for the manufacture of geopolymer-based products, Waste Manag. 28 (2008) 416–423.
[36] W.P. Linak, C.A. Miller, W.S. Seames, J.O.L. Wendt, T. Ishinomori, Y. Endo, S. Miyamae, On trimodal particle size distributions in fly ash from pulverized–coal combustion, Proc. Combust. Inst. 29 (2002) 441–447.